1987-09-01

Energy and angular distributions of Rh atoms ejected due to ion bombardment from Rh{111}: A theoretical study

Garrison, Barbara J.

American Physical Society

PHYSICAL REVIEW B VOLUME 36, NUMBER 7 1 SEPTEMBER 1987

Energy and angular distributions of Rh atoms ejected due to ion bombardment from Rh{111}: A theoretical study

Barbara J. Garrison, Curt T. Reimann, and Nicholas Winograd
Department of Chemistry, 152 Davey Laboratory, The Pennsylvania State University, University Park, Pennsylvania 16802

Don E. Harrison, Jr.
Department of Physics and Chemistry, Naval Postgraduate School, Monterey, California 93943
(Received 23 March 1987)

Energy and angular distributions of Rh atoms ejected from a Rh{111} surface due to keV ion bombardment are predicted from classical dynamics calculations and are compared to those measured using a multiphoton resonance ionization scheme. The comparison is generally quite favorable. For example, the calculated distributions reproduce the changes in azimuthal anisotropy which occur over an ejected-particle kinetic energy range of 5–50 eV. The new detailed experimental data do, however, expose deficiencies in the pair potential, which we believe can be overcome with a many-body potential.

I. INTRODUCTION

Numerous experimental and theoretical investigations of the energy and angular distributions of atoms and molecules ejected from single-crystal surfaces due to keV ion bombardment have been made over the years. Wehner was the first to observe "spots," or anisotropic angular distributions,[1] which are closely related to the surface structure. His method of detection unfortunately did not allow him to mass or energy filter the ejected species. More recently, energy and angular distributions of ions have been measured by quadrupole mass detectors.[2–4] These data are energy, mass, and angle resolved but are characteristic of the desorbed ionic species. The theoretical investigations, mainly computer simulations, on the other hand, predict the distributions of the neutral species.[5–8] Comparisons between the predicted neutral distributions and the measured ion distributions have been qualitatively and semiquantitatively favorable.[2–4] However, it is difficult to make rigorous quantitative comparisons since the velocity and angle dependence of the ionization probability are not known and since the ions experience a different interaction potential (e.g., image force) than the neutrals as they leave the surface. Thus the final ion distributions are shifted from the neutral ones.[9] It would be advantageous to be able to directly compare experimental and theoretical distributions in order to generate a standard and realistic model for describing the ion-solid interaction. This model can then be used to (i) gain structural information about the surface from the measured energy and angular distributions and (ii) learn more about the details of the sputtering process.

For the first time energy- and angle-resolved neutral (EARN) distributions have been obtained for Rh atoms ejected from clean and oxygen-covered Rh{111} surfaces due to Ar^+-ion bombardment.[10–12] In this study a classical dynamics model has been used to compute the predicted EARN distributions. The polar-angle distributions of the ejected Rh atoms from normally incident Ar^+ bombardment are analyzed for three azimuthal angles of ejection and three energy ranges. The calculated distributions exhibit the same azimuthal anisotropy as the experimental curves including the transition from a threefold azimuthal pattern at low Rh atom energies to an approximately sixfold pattern in the energy range 20–50 eV. In addition, in both the experimental and calculated distributions the intensity in the direction normal to the surface increases relative to the peak intensity at a polar angle of 30°–40° as the secondary-particle energy increases. The predicted distributions are in excellent overall agreement with the experimental ones except for two features. (i) The predicted peak position in the polar distribution is $\sim 5°–15°$ closer to the surface normal than the experimental peak. (ii) The calculated peak position in the energy distribution is at approximately one-half the experimental value. The fact that there is global agreement between the calculated and experimental results indicates that the classical dynamics model incorporates the essential physics of the ion-bombardment process. From the discrepancies between the two sets of distributions we will identify the important neglected interactions.

II. DESCRIPTION OF THE CALCULATION

A classical dynamics prescription is used to model the keV-ion-bombardment events. A microcrystallite array of atoms approximates a single-crystal substrate. The primary particle, whose energy and angle of incidence are known, is aimed at the surface. The subsequent movements of all the atoms are then determined by integrating Hamilton's equations of motion. The final momenta of the sputtered species are used to calculate the energy and angles of the ejected Rh atoms. A complete description of the calculational procedure has been given elsewhere.[13–15]

The experimental condition is that normally incident 5-keV Ar^+ ions bombard a Rh{111} crystal.[10–12] To model 5-keV bombardment and describe most of the ejection events would require a sample of atoms[15] larger than

TABLE I. Potential parameters.

	A (keV)	B (Å^{-1})	D_e (eV)	R_e (Å)	α (Å^{-1})	R_a (Å)	R_b (Å)	R_c (Å)
Rh-Rh	54.33	5.088	0.8237	2.75	1.56	1.33	1.62	4.56
O-O			5.21	1.21	2.65			4.56
Rh-O			0.90	1.95	2.00			4.56
C site								
Rh-O			1.79	1.95	2.00			4.56
Atop								

is computationally feasible at this time. Therefore, the energy of the Ar particle is reduced to 3 keV in the calculations. Even with this lower energy a crystallite with a minimum of ~ 108 Rh atoms per layer (Fig. 1) and five layers deep is necessary to modestly contain the ejection process. For the simulation on clean Rh{111} 1000 Ar impacts on the surface were calculated. With this size crystallite each Ar impact takes ~ 4 min of computer time on a Floating Point Systems 5205 Array Processor. To ultimately make detailed comparisons of calculated and measured distributions, it is desirable to have a lower energy (500–1000 eV) Ar^+ beam so that smaller crystallites are appropriate.

To reproduce the experimental configuration an average over all possible Ar^+-ion impact positions on the surface is performed. For a clean {111} face this corresponds to the normally incident Ar particle being aimed within the triangular region shown in the center of Fig. 1. In addition to clean Rh{111}, a $p(2\times 2)$ overlayer of oxygen atoms on the same surface is modeled. Two adsorption sites, the "atop" site (O atom directly above a Rh atom) and the C site (O atom above a third-layer metal atom) are considered. The C-site positions of atoms are shown in Fig. 1. In the atop configuration the height of the oxygen atom is 1.95 Å above the surface plane and for the C-site configuration the height is 1.185 Å. These values were chosen to maintain a constant Rh-O nearest-neighbor distance of 1.95 Å, a value which was determined by adding the approximate atomic radii of Rh and O atoms. This value for the C-site height is slightly less than the value (1.23 Å) reported recently by Wong *et al.*[16] For the $p(2\times 2)$ oxygen overlayer the symmetry region for the Ar bombardment is 4 times larger than that of the clean Rh{111} surface.

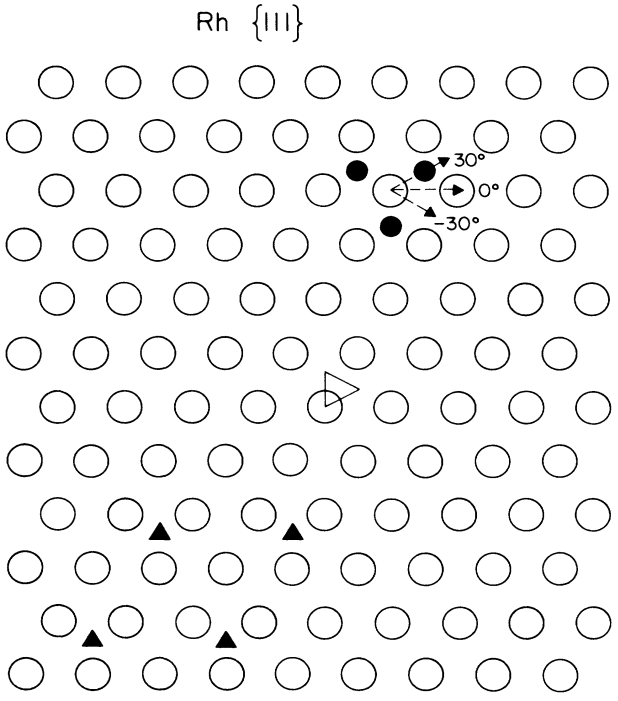

FIG. 1. Rh{111} crystal face. The triangle in the center is the irreducible symmetry zone for ion impacts at normal incidence on clean Rh{111}. The solid circles show the placement of the second layer atoms. The solid triangles show a portion of the lateral positions of the C-site oxygen atoms. The azimuthal direction, ϕ, is shown in the upper right-hand corner.

A critical assumption in any scattering calculation involves the nature of the forces among the particles. In previous simulations a best estimate of the forces or interaction potentials has been made, but real understanding of the forces, especially in the low-energy regime, is limited. It is hoped that eventually, in conjunction with EARN experiments, significant advances in knowledge of the interaction potential can be made. In all cases discussed here the potentials are expressed as a sum of pairwise interactions. For the Ar-Rh and Ar-O interactions, a Moliere potential with the Thomas-Fermi screening radius is used,[17] 0.095 and 0.127 Å for Ar-Rh and Ar-O, respectively. For the Rh-Rh interaction, $V(R)$, a composite pair potential of the form

$$V(R)=\begin{cases} A\,e^{-BR}, & R<R_a \quad (1)\\ \text{cubic spline}, & R_a<R<R_b \quad (2)\\ D_e e^{-\alpha(R-R_e)}(e^{-\alpha(R-R_e)}-2), & R_b<R<R_c \quad (3)\\ 0, & R>R_c \quad (4)\end{cases}$$

where R is the internuclear separation between the pair of atoms, is used. The values of all the parameters are given in Table I. The Rh-Rh Morse parameters were obtained by fitting to the bulk heat of atomization (5.76 eV),[18] the lattice constant (3.804 Å),[19] and the bulk compressibility (3.69×10^{-13} cm^2/dyn).[20] The Rh-Rh exponential repulsive wall [Eq. (1)] is similar in size to a Moliere function[17] with a Thomas-Fermi screening length (0.083 Å). For the Rh-O and O-O interactions the Morse potential [Eq. (3)] is used for all separations less than R_c.

III. RESULTS AND DISCUSSION

The energy and angle distributions of the sputtered Rh atoms can be displayed in numerous ways. Our choice here is to compare polar-angle distributions for fixed secondary particle energy and azimuthal angle. The resulting displays are shown in Figs. 2 and 3. In all cases the polar angle is denoted by θ and is measured from the surface normal. The azimuthal angle is ϕ and the three high-symmetry directions are shown in the upper right-hand corner of Fig. 1. The experimental data have been provided by Winograd and co-workers[21] and is equivalent to that given in Ref. 12. The details of the averaging procedure will be discussed in a forthcoming paper on the EARN distributions from O/Rh{111} systems.

As seen in Fig. 2, there is semiquantitative agreement between the calculated and measured distributions. The azimuthal anisotropy is correctly predicted for all energy ranges. The intensity is higher along the open surface directions ($\phi=\pm30°$) than along the close-packed azimuth ($\phi=0°$). If only the surface structure influenced the distributions, an azimuthal pattern should result with the distributions at $\phi=\pm30°$ being equivalent. Results from the calculations, the experiments discussed here,[10–12] and many previous experiments[22,23] exhibit distributions with the intensity along $\phi=-30°$ being greater than at $\phi=30°$, indicating that subsurface scattering events are important in the ejection process. Both theory and experiment indicate that the intensity at $\theta=0°$ ("center spot") relative to the peak intensity at $\theta=25°$–$40°$ increases as the Rh-atom energy increases.

The major discrepancy between theory and experiment involves the position and width of the peak at 20°–35° ("the spot"). The calculated peak position is ~5°–15° closer to the normal direction than the experimental peak. In addition, the experimental peaks are broader.

Upon examining the collision sequences that give rise to the ejection of Rh atoms, it is apparent that there are *many* reasons that the intensity at $\phi=\pm30°$ is larger than at $\phi=0°$. (i) The surface atoms can focus an exiting first-layer atom on the outward path into $\phi=\pm30°$. (ii) The first-layer atoms can focus a moving atom downward along $\phi=\pm30°$, where it reflects off a second-layer atom and knocks out a first-layer atom. (iii) Variations and combinations of the above with other-layer atoms also occur. *There can be both upward and downward alignment of the atomic motion,* all of which lead to preferential ejection along the azimuths of $\pm30°$.

Given the multitude of different collision sequences that result in the ejection of atoms into $\phi=\pm30°$, it is somewhat difficult to extract the essential reasons for the higher intensity at $\phi=-30°$ than at $\phi=30°$. Upon careful analysis of the collision sequences the following mechanism appears to be the important factor. In the geometry of the {111} surface (Fig. 1), the second-layer atoms are positioned such that if a second-layer atom moves towards the surface in the $-30°$ direction, it hits a first-layer atom. From the first-layer atom's point of view, there is a second-layer atom that can knock it out along the $-30°$ azimuth, but not along the $+30°$ azimuth. From this experimental data, these calculations, and other experimental data, the magnitude of the $\pm30°$ anisotropy is observed to be dependent on the substrate type, the pri-

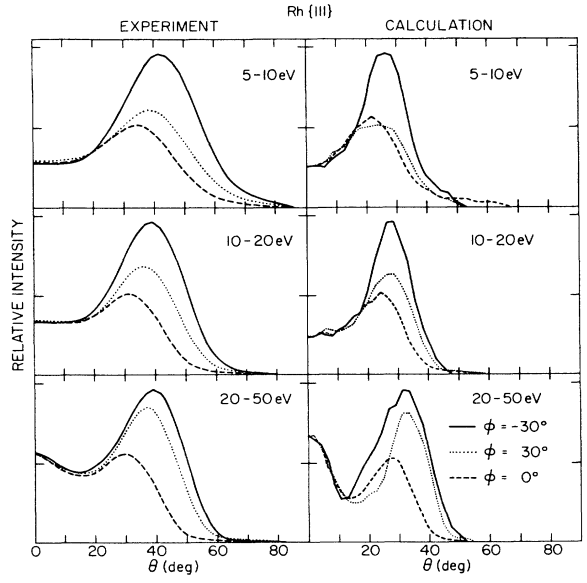

FIG. 2. Polar-angle distributions for various azimuthal angles for fixed secondary kinetic energy of the Rh atoms. In each frame the data are normalized to the $\phi=-30°$ peak intensity. For the calculated data the full width at half maximum of the resolution is 15° in the polar direction. A constant solid angle is used in the histogramming procedure. The experimental resolution is approximately the same. The surface normal corresponds to $\theta=0°$.

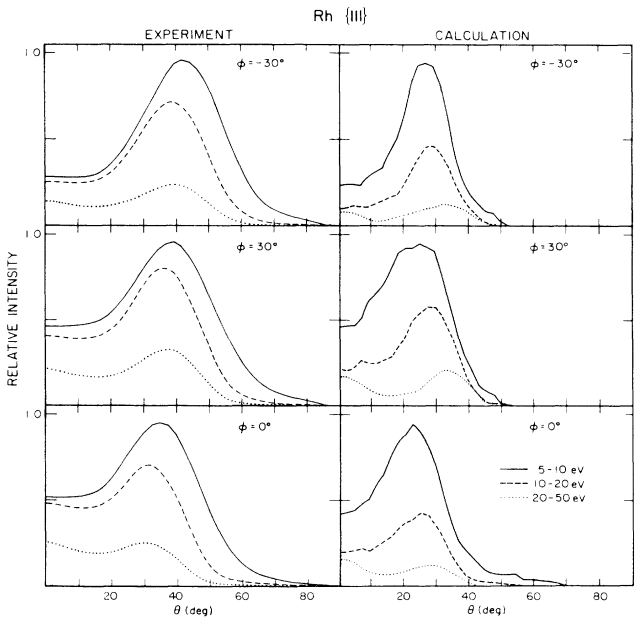

FIG. 3. Polar-angle distributions for various secondary kinetic energies for fixed azimuthal angle of the Rh atoms. In each frame the raw data are divided by the width of the energy window and then normalized to the 5–10 eV peak intensity.

mary ion energy and mass, the energy of the sputtered particle, and the potentials used in the calculation.

The polar distributions for fixed azimuthal angle and various secondary particle energy ranges are shown in Fig. 3. Again, the overall agreement between the corresponding sets of experimental and calculated curves is quite good. However, the calculated intensities in the (10–20)- and (20–50)-eV ranges are too low with respect to the (5–10)-eV intensity. This difference is more pronounced in Fig. 4, where the experimental and calculated energy distributions are shown.

The experimental energy distributions are shown in Fig. 4 for (i) all polar and azimuthal angles, (ii) the high-intensity direction ($\theta=40°, \phi=-30°$), and (iii) the direction normal to the surface ($\theta=0°$). The calculated distributions are given for (i) all angles and (ii) the high-intensity direction ($\theta=28°, \phi=-30°$). In the experimental curves the energy distribution for all angles maximizes at ~ 4 eV with the peaks in both the "spot" and "center spot" directions at higher energies. The distribution in the direction normal to the surface has more intensity at $E=20$ eV than the other two curves. The value of the energy at the maximum in the calculated distributions is at approximately one-half the experimental values. The energy distribution in the "spot" is considerably broader than that for all angles. The distribution normal to the surface (not shown) does not appear visually that different from the others, but as discussed below, we can extract some mechanistic information from it.

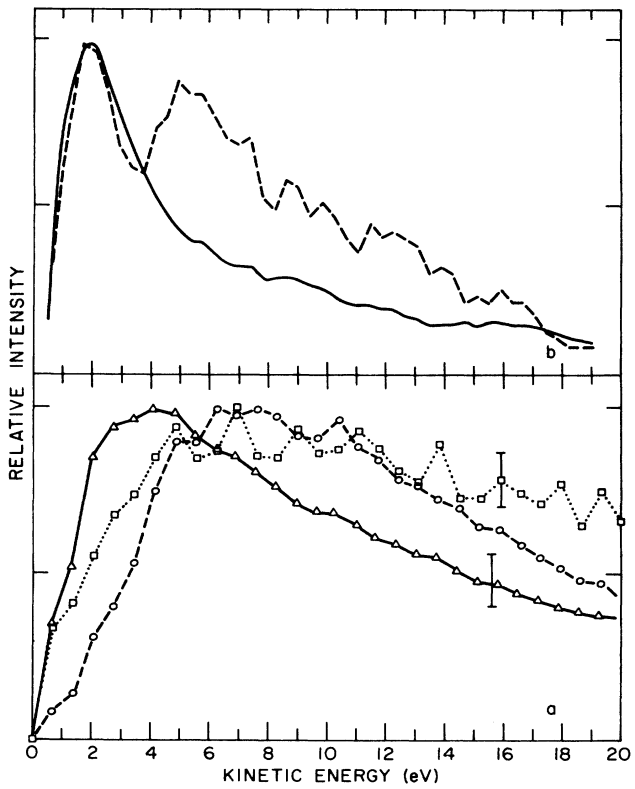

FIG. 4. Experimental and calculated kinetic energy distributions. In all cases the curves are peak normalized. (a) Experimental. The error bars indicate both counting statistics and reproducibility in data collection. All particles (solid line); $\theta=40°\pm3°$, $\phi=-30°$ (dashed line); $\theta=0°\pm7.5°$ (dotted line). (b) Calculated. All particles (solid line); $\theta=28°\pm3°$, $\phi=-30°$ (dashed).

The peak positions in the experimental curves occur at 0.7–1.25 times the heat of sublimation of rhodium metal. These values are consistent with those reported for polycrystalline Rh samples[24,25] and they correspond to the idea that the peak energy is the true energy cost to remove an atom from the solid[26,27] and not half the heat of sublimation as proposed by Thompson.[28] The fact that the calculated value is too low is disturbing and is currently being investigated.

The reason for the relatively large intensity at $E=20$ eV in the $\theta=0°$ curve can be extracted by following individual collision sequences and noting the initial site of each ejected atom. With a primary ion energy of 3 keV, considerable energy is deposited deeply within the crystal. It is possible for the primary ion to find a channel and penetrate to the third layer or below without undergoing any hard collisions with first- or second-layer atoms. Subsequently, there can be hard collisions with ion reflection well below the surface, so that second-layer atoms can be hit from behind and directed straight up through the threefold holes. From the simulations the center spot has a large second layer contribution. It also has a relatively more intense high energy tail than found at other angles (slightly discernible in the calculated distributions). We would expect this second layer component to be strongly dependent on the primary ion energy. The observation that second layer ejected atoms have higher energies has been reported recently by Shapiro *et al.*, for sputtering from Cu{100} crystals.[29]

Finally, calculated angular distributions with a $p(2\times2)$ oxygen atom overlayer in both atop- and *C*-site configurations are compared to experimental distributions in Fig. 5. There appears to be "better" agreement between the *C*-site results and experimental data than between the atop-site results and the data. This conclusion is consistent with recent low-energy electron-diffraction results given in Ref. 16. However, given the uncertainties in the simulations of the bombardment of clean Rh{111}, it is not possible to ascertain the O-atom position from these calculations. Of note is that the angular distributions of the Rh atoms depend on the positions of the oxygen atoms.

Several efforts were made to improve the agreement between the calculated and experimental EARN distributions. The major criterion in deciding whether we had "improved" the calculation was whether the peak position and width of the energy distribution approached the experimental values. Temperature effects were incorporated by choosing the initial surface-atom positions from a Gaussian distribution centered at the equilibrium site with a width derived from the Debye-Waller factor and the temperature. Within the statistical uncertainty, finite temperature had no effect on the results of the simulation. Inelastic effects were incorporated by inclusion of a friction term in the equations of motion.[30] Although the overall yield decreased, the shape of the energy distribu-

tion did not change. Larger and smaller Rh-Rh pair potentials in the (5–100)-eV region were used. This resulted in shifts of the peak positions in the polar distribution and changes in the azimuthal anisotropy, but did not alter the energy distribution. Finally, larger values of D_e and consequently larger surface binding energies were used. By doubling D_e the peak of the energy distribution was moved to approximately the correct position, but the width was still too narrow. We do not believe this alteration in the binding energy to be justified physically, so we do not consider this an improvement in the model. Many of these variations changed features of the calculated distributions, but none made any significant improvement and some made the agreement worse.

IV. CONCLUSIONS

The energy and angular distributions of Rh atoms ejected due to keV ion bombardment of a Rh{111} crystal have been calculated by a classical dynamics model and compared to the experimentally measured quantities. The overall agreement between the two sets of distributions is remarkable except for the positions of the peak in both the polar and energy distributions. Preliminary experimental and calculated Rh-atom distributions from an oxygen-covered Rh{111} surface show that the angular distributions are sensitive to adsorbate position.

In the present study it is gratifying that the majority of the features in the EARN distributions are well reproduced and explained utilizing simple pairwise additive potentials. There are, however, deficiencies in the model that have been exposed by the EARN data. The problem appears to be the interaction potential and work is underway[31] to include the many-body embedded-atom potential of Daw and Baskes.[32] Preliminary results using this potential yield calculated energy distributions that reproduce the peak position and width of the experimental values. In addition, the positions of the peaks in the polar distributions increase by $\sim 5°-10°$. We are optimistic that with this new detailed EARN data, accurate potentials can be developed for describing the ion-bombardment events.

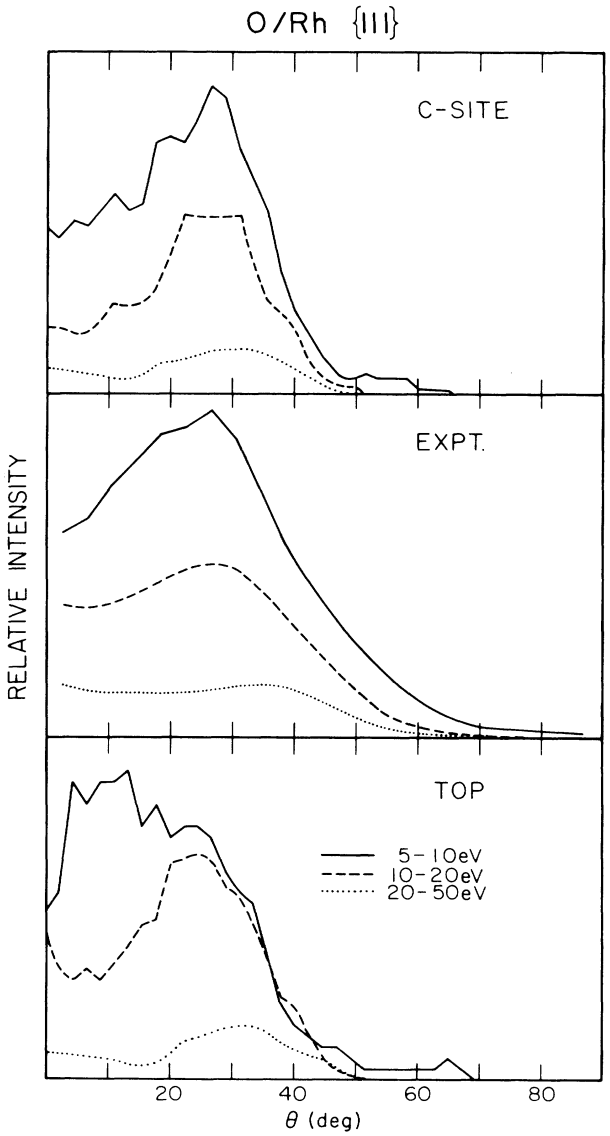

FIG. 5. Polar-angle distributions of Rh atoms from a surface with a $p(2\times2)$ overlayer of oxygen. In all cases the azimuthal angle is $-30°$.

ACKNOWLEDGMENTS

This work was greatly enhanced by discussions with J. Baxter, M. El-Maazawi, P. Kobrin, D. Lo, A. Schick, M. Shapiro, J. Singh, T. Tombrello, and K. Walzl. The financial support of the National Science Foundation, The U.S. Office of Naval Research, the U.S. Air Force Office of Scientific Research, the Foundation Research Program of the Naval Postgraduate School, the IBM Corporation, and the Camille and Henry Dreyfus Foundation is gratefully acknowledged.

[1]G. K. Wehner, Phys. Rev. **102**, 690 (1956).
[2]S. P. Holland, B. J. Garrison, and N. Winograd, Phys. Rev. Lett. **43**, 220 (1979).
[3]R. A. Gibbs, S. P. Holland, K. E. Foley, B. J. Garrison, and N. Winograd, Phys. Rev. B **24**, 6178 (1981).
[4]R. A. Gibbs, S. P. Holland, K. E. Foley, B. J. Garrison, and N. Winograd, J. Chem. Phys. **76**, 684 (1982).
[5]D. E. Harrison, Jr., J. P. Johnson III, and N. S. Levy, Appl. Phys. Lett. **8**, 33 (1966).
[6]N. Winograd, B. J. Garrison, and D. E. Harrison, Jr., Phys. Rev. Lett. **41**, 1120 (1978).
[7]R. P. Webb, Radiat. Effects **89**, 234 (1985).
[8]S. Kapur and B. J. Garrison, J. Chem. Phys. **75**, 445 (1981); Surf. Sci. **109**, 435 (1981).

[9]B. J. Garrison, Surf. Sci. Lett. **167**, L225 (1986).
[10]J. P. Baxter, G. A. Schick, J. Singh, P. H. Kobrin, and N. Winograd, J. Vac. Sci. Technol. **4**, 1218 (1986).
[11]G. A. Schick, J. P. Baxter, J. Singh, P. H. Kobrin, and N. Winograd, in *Secondary Ion Mass Spectrometry—SIMS V*, Vol. 44 of *Springer Series in Chemical Physics*, edited by A. Benninghoven, R. J. Colton, D. S. Simons, and H. W. Werner (Springer, New York, 1986), p. 90.
[12]N. Winograd, P. H. Kobrin, G. A. Schick, J. Singh, J. P. Baxter, and B. J. Garrison, Surf. Sci. Lett. **176**, 1817 (1986).
[13]N. Winograd, Prog. Solid State Chem. **13**, 285 (1982).
[14]B. J. Garrison and N. Winograd, Science **216**, 805 (1982).
[15]D. E. Harrison, Jr. and M. M. Jakas, Radiat. Effects **91**, 263 (1986); D. E. Harrison, Jr., in *Proceedings of the Symposium on Sputtering*, edited by P. Varga *et al.* (Perchtoldsdorf, Vienna, Austria, 1980), p. 36.
[16]P. C. Wong, K. C. Hui, M. Y. Zhan, and K. A. R. Mitchell, Surf. Sci. **165**, L21 (1986).
[17]I. M. Torrens, *Interatomic Potentials* (Academic, New York, 1972).
[18]*CRC Handbook of Chemistry and Physics*, 59th ed., edited by R. C. Weast (CRC, West Palm Beach, FL, 1978).
[19]N. W. Ashcroft and N. D. Mermin, *Solid State Physics* (Saunders College, Philadelphia, 1976).
[20]C. Kittel, *Introduction to Solid State Physics*, 5th ed. (Wiley, New York, 1976).
[21]N. Winograd, C. T. Reimann, M. El-Maazawi, and K. Walzl (unpublished).
[22]W. Szymczak and K. Wittmaack, in *Proceedings of the Symposium on Sputtering*, Ref. 18, p. 236.
[23]R. G. Musket and H. P. Smith, Jr., J. Appl. Phys. **39**, 3579 (1968).
[24]J. P. Baxter, J. Singh, G. A. Schick, P. H. Kobrin, and N. Winograd, Nucl. Instrum. Methods B **17**, 300 (1986).
[25]B. J. Garrison, Nucl. Instrum. Methods B **17**, 305 (1986).
[26]B. J. Garrison, N. Winograd, D. Lo, T. A. Tombrello, M. H. Shapiro, and D. E. Harrison, Jr., Surf. Sci. Lett. **180**, L129 (1987).
[27]R. Oliva, R. Kelly, and G. Falcone, Nucl. Instrum. Methods B **19-20**, 101 (1987).
[28]M. W. Thompson, Philos. Mag. **18**, 377 (1968).
[29]M. H. Shapiro, P. K. Haff, T. A. Tombrello, D. E. Harrison, Jr., and R. P. Webb, Radiat. Effects **89**, 243 (1985).
[30]J. Lindhard, V. Nielsen, M. Sharff, and P. V. Thomsen, Kgl. Dansk. Vidensk. Selsk. Mat.-Fys. Medd. **33**, No. 10 (1963).
[31]B. J. Garrison, N. Winograd, D. Lo, T. A. Tombrello, M. H. Shapiro, and D. E. Harrison, Jr. (unpublished).
[32]M. S. Daw and M. I. Baskes, Phys. Rev. Lett. **50**, 1285 (1983); Phys. Rev. B **29**, 6443 (1984).